

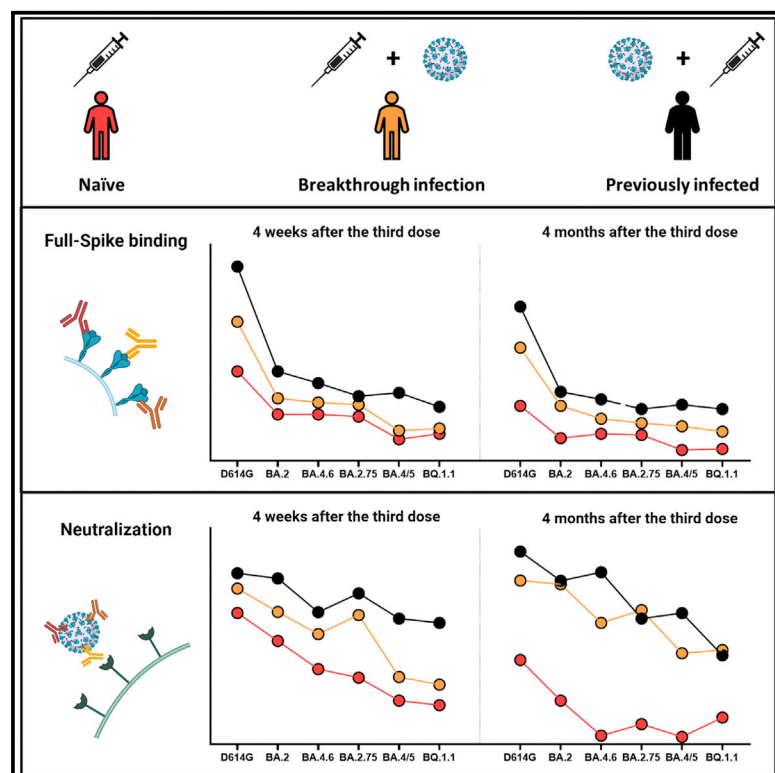


Since January 2020 Elsevier has created a COVID-19 resource centre with free information in English and Mandarin on the novel coronavirus COVID-19. The COVID-19 resource centre is hosted on Elsevier Connect, the company's public news and information website.

Elsevier hereby grants permission to make all its COVID-19-related research that is available on the COVID-19 resource centre - including this research content - immediately available in PubMed Central and other publicly funded repositories, such as the WHO COVID database with rights for unrestricted research re-use and analyses in any form or by any means with acknowledgement of the original source. These permissions are granted for free by Elsevier for as long as the COVID-19 resource centre remains active.

Spike recognition and neutralization of SARS-CoV-2 Omicron subvariants elicited after the third dose of mRNA vaccine

Graphical abstract



Authors

Alexandra Tauzin, Alexandre Nicolas, Shilei Ding, ..., Marceline Côté, Renée Bazin, Andrés Finzi

Correspondence

andres.finzi@umontreal.ca

In brief

Tauzin et al. report that while the third dose of mRNA vaccine induces poor humoral responses against new Omicron subvariants in naive people, better responses are observed in individuals with hybrid immunity. They also observe that BA.4/5 and BQ.1.1 are less recognized and neutralized than other Omicron subvariants.

Highlights

- In naive donors, the boost induces poor humoral responses against Omicron variants
- Hybrid immunity generates better humoral responses than vaccination alone
- BA.4/5 and BQ.1.1 spikes are more resistant than other Omicron subvariants



Report

Spike recognition and neutralization of SARS-CoV-2 Omicron subvariants elicited after the third dose of mRNA vaccine

Alexandra Tauzin,^{1,2} Alexandre Nicolas,^{1,2,10} Shilei Ding,^{1,10} Mehdi Benlarbi,^{1,2} Halima Medjahed,¹ Debashree Chatterjee,¹ Katrina Dionne,^{1,2} Shang Yu Gong,^{1,3} Gabrielle Gendron-Lepage,¹ Yuxia Bo,⁴ Josée Perreault,⁵ Guillaume Goyette,¹ Laurie Gokool,¹ Pascale Arlotto,¹ Chantal Morrisseau,¹ Cécile Tremblay,^{1,2} Valérie Martel-Laferrrière,^{1,2} Gaston De Serres,⁶ Inès Levade,⁷ Daniel E. Kaufmann,^{1,8,9} Marceline Côté,⁴ Renée Bazin,⁵ and Andrés Finzi^{1,2,3,11,*}

¹Centre de Recherche du CHUM, Montreal, QC H2X 0A9, Canada

²Département de Microbiologie, Infectiologie et Immunologie, Université de Montréal, Montreal, QC H2X 0A9, Canada

³Department of Microbiology and Immunology, McGill University, Montreal, QC H3A 2B4, Canada

⁴Department of Biochemistry, Microbiology and Immunology, and Centre for Infection, Immunity, and Inflammation, University of Ottawa, Ottawa, ON K1H 8M5, Canada

⁵Héma-Québec, Affaires Médicales et Innovation, Quebec, QC G1V 5C3, Canada

⁶Institut National de Santé Publique du Québec, Quebec, QC H2P 1E2, Canada

⁷Laboratoire de Santé Publique du Québec, Institut National de Santé Publique du Québec, Sainte-Anne-de-Bellevue, QC H9X 3R5, Canada

⁸Département de Médecine, Université de Montréal, Montreal, QC H3T 1J4, Canada

⁹Division of Infectious Diseases, Department of Medicine, University Hospital of Lausanne and University of Lausanne, 1011 Lausanne, Switzerland

¹⁰These authors contributed equally

¹¹Lead contact

*Correspondence: andres.finzi@umontreal.ca

<https://doi.org/10.1016/j.celrep.2023.111998>

SUMMARY

Several severe acute respiratory syndrome coronavirus 2 (SARS-CoV-2) Omicron subvariants have recently emerged, becoming the dominant circulating strains in many countries. These variants contain a large number of mutations in their spike glycoprotein, raising concerns about vaccine efficacy. In this study, we evaluate the ability of plasma from a cohort of individuals that received three doses of mRNA vaccine to recognize and neutralize these Omicron subvariant spikes. We observed that BA.4/5 and BQ.1.1 spikes are markedly less recognized and neutralized compared with the D614G and other Omicron subvariant spikes tested. Also, individuals who have been infected before or after vaccination present better humoral responses than SARS-CoV-2-naïve vaccinated individuals, thus indicating that hybrid immunity generates better humoral responses against these subvariants.

INTRODUCTION

The severe acute respiratory syndrome coronavirus 2 (SARS-CoV-2) Omicron variant BA.1 emerged at the end of 2021 and rapidly became the dominant circulating strain in the world.^{1,2} Since its emergence, several sublineages of Omicron have rapidly replaced the BA.1 variant due to higher transmission rates. BA.2 became the dominant circulating strain in spring 2022,^{3,4} and currently, the BA.4 and BA.5 variants (sharing the same mutations in their spike glycoproteins, named BA.4/5 S in the report) are the dominant circulating strains in several countries.^{5–8} BA.2.75, BA.4.6, and BQ.1.1 have emerged more recently and are spreading worldwide.^{9,10}

It was previously shown that poor humoral responses against BA.1 and BA.2 variants were observed after two doses of mRNA vaccine.^{11–13} We and other reported that an extended interval

between the first two doses of mRNA vaccine led to strong humoral responses to several variants of concern (VOCs) including BA.1 and BA.2 after the second dose of mRNA vaccine.^{14–16}

However, a third dose of mRNA vaccine led to an increase of humoral responses against these Omicron variants regardless of the interval between doses.^{11,13,16,17} Previous studies also reported that breakthrough infection (BTI) in vaccinated people induced strong neutralizing antibodies (Abs) against VOCs, including BA.1.^{18,19} However, recent studies have shown that BA.4/5, BA.2.75, BA.4.6, and BQ.1.1 appear to be more resistant than BA.1 and BA.2 to antibodies elicited by vaccination and monoclonal Abs.^{20–26}

In this study, we analyzed the ability of plasma from vaccinated individuals to recognize and neutralize pseudoviral particles bearing different Omicron subvariant spikes 4 weeks (median [range]: 30 days [20–44 days]) and 4 months (median



Table 1. Characteristics of the vaccinated SARS-CoV-2 cohorts

	Entire cohort	Naive	Breakthrough infection ^a	Previously infected
Number	45	15	15	15
Age	51 (24–67)	54 (24–67)	43 (30–64)	48 (29–65)
Gender	male (n)	4	5	8
	female (n)	28	11	7
Vaccine	first dose	Pfz = 43; M = 1; AZ = 1	Pfz = 14; M = 1	Pfz = 14; AZ = 1
	second dose	Pfz = 43; M = 1; AZ = 1	Pfz = 14; M = 1	Pfz = 14; AZ = 1
	third dose	Pfz = 40; M = 5	Pfz = 15	Pfz = 14; AZ = 1
Days between symptom onset and the first dose ^b	N/A	N/A	N/A	288 (166–321)
Days between the first and second dose ^b	110 (54–146)	109 (65–120)	110 (54–113)	112 (90–146)
Days between the second and third dose ^b	211 (151–235)	210 (184–227)	215 (151–224)	219 (187–235)
Days between the third dose and 4 weeks	30 (20–44)	32 (21–37)	28 (20–38)	33 (24–44)
Days between the third dose and 4 months	121 (92–135)	124 (105–135)	121 (92–131)	119 (111–127)

Pfz, Pfizer/BioNTech BNT162b2; M, Moderna mRNA-1273; AZ, AstraZeneca ChAdOx1.

^aAll breakthrough infection individuals were infected between mid-December 2021 and May 2022, when almost only Omicron variants (BA.1 and BA.2) were circulating in Quebec. 6 breakthrough infection (BTI) individuals were infected before the time point collected 4 weeks after the third dose, and 9 BTI individuals were infected between the two time points.

^bValues displayed are medians, with ranges in parentheses. Continuous variables were compared by using Kruskal-Wallis tests. $p < 0.05$ was considered statistically significant for all analyses. No statistical differences were found for any of the parameter tested between the different groups.

[range]: 121 days [92–135 days]) after the third dose of mRNA vaccine. This study was conducted in a cohort of individuals who received their first two doses with a 16-week extended interval (median [range]: 110 days [54–146 days]) and their third dose 7 months after the second dose (median [range]: 211 days [151–235 days]). The cohort included 15 naive individuals who were never infected with SARS-CoV-2, 15 previously infected (PI) individuals who were infected during the first wave of COVID-19 in early 2020 (before the advent of the Alpha variant and other VOCs) and before vaccination, and 15 BTI individuals who were infected after vaccination. All BTI individuals were infected between mid-December 2021 and May 2022, when almost only Omicron variants (BA.1 and BA.2) were circulating in Quebec. Basic demographic characteristics of the cohorts and detailed vaccination time points are summarized in Table 1 and Figure 1A.

RESULTS

RBD-specific IgG and associated avidity

We first measured the level of anti-receptor-binding-domain (RBD) immunoglobulin G (IgG) 4 weeks and 4 months after the third dose of mRNA vaccine in naive, BTI, and PI individuals (Figure 1A) by a well-described ELISA assay^{16,27–30} (Figure 1B). Four weeks after the third dose, we did not observe significant differences in the level of IgG between the three groups. Four months after the third dose, we observed that the level of IgG significantly decreased in all groups but decreased to a higher extent in naive individuals. No significant differences were observed between naive, BTI, and PI individuals 4 months after the boost. We also measured the avidity of anti-RBD IgG induced after the third dose of mRNA vaccine using a previously described assay.^{28,31} Four weeks after the third dose, we observed that naive donors had IgG with lower avidity,

although we only measured a significant difference with BTI individuals (Figure 1C). Four months after the third dose, the avidity of these IgG slightly decreased for naive individuals but remained stable for BTI and PI groups.

RBD-specific B cell responses after the third dose of mRNA vaccine

We also monitored the SARS-CoV-2-specific B cells (identified as CD19+ CD20+) by flow cytometry using two recombinant RBD protein probes labeled with two different fluorochromes (Alexa Fluor 594 and Alexa Fluor 488) (Figure S1A).^{30,32} Four weeks after the third dose of mRNA vaccine, no significant differences in the level of circulating B cells were observed between the three groups (Figure 1D). Four months after the boost, this level significantly decreased for naive donors but not for individuals with hybrid immunity (PI and BTI). For BTI individuals, we observed an increase, with some donors presenting a higher level of circulating RBD-specific B cells, probably due to recent infection.

Recognition of SARS-CoV-2 spike variants by plasma from vaccinated individuals

We next measured the ability of plasma to recognize the SARS-CoV-2 D614G and different Omicron subvariant spikes in vaccinated naive, PI, and BTI individuals 4 weeks and 4 months after the third dose of mRNA vaccine. Spike expression levels of the spike variants were normalized to the signal obtained with the conformationally independent anti-S2 neutralizing CV3-25 Ab^{33–35} that efficiently recognized all these spikes despite their various mutations (Figures S1B and S2A–S2C). Four weeks after the third dose of mRNA vaccine, we observed that plasma from PI individuals recognized more efficiently the D614G spike than naive individuals (Figure 2A). We also observed that BTI individuals recognized the D614G spike as efficiently as the PI individuals. Four months after the third dose, the level of

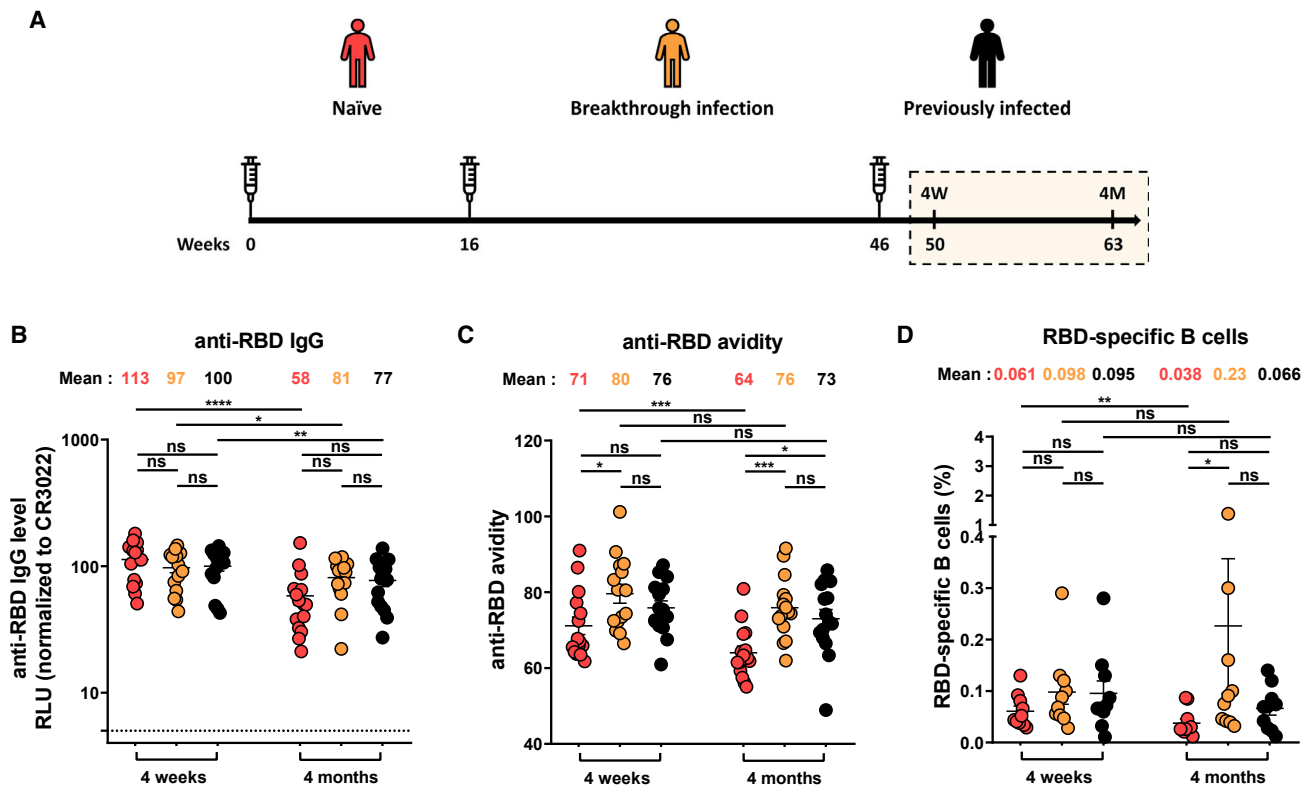


Figure 1. Anti-RBD IgG level, associated anti-RBD avidity, and RBD-specific B cell responses in plasma from naive, BTI, and PI individuals after the third dose of mRNA vaccine

(A) SARS-CoV-2 vaccine cohort design. The yellow box represents the period under study.

(B and C) Indirect ELISAs were performed by incubating plasma samples from naive, BTI, or PI individuals collected 4 weeks or 4 months after the third dose of mRNA vaccine with recombinant SARS-CoV-2 RBD protein. Anti-RBD Ab binding was detected using HRP-conjugated anti-human IgG.

(B) RLU values obtained were normalized to the signal obtained with the anti-RBD CR3022 mAb present in each plate.

(C) The RBD avidity index corresponded to the value obtained with the stringent (8 M urea) ELISA divided by that obtained without urea.

(D) The frequencies of RBD+ B cells were measured by flow cytometry.

(B–D) Plasma samples were grouped in two different time points (4 weeks and 4 months).

Naive, BTI, and PI individuals are represented by red, yellow, and black points, respectively, undetectable measures are represented as white symbols, and limits of detection are plotted. Error bars indicate means \pm SEM (* $p < 0.05$; ** $p < 0.01$; *** $p < 0.001$; **** $p < 0.0001$; ns, non-significant). For all groups, $n = 15$ (B and C) or $n = 10$ (D).

recognition of the D614G spike decreased for the three groups but with a more significant reduction in the naive group. For the BA.2, BA.4/5, and BQ.1.1 spikes, naive and BTI individuals had the same level of recognition 4 weeks after the third dose, and this level was significantly lower than for PI individuals (Figures 2B–2C and 2F). For BA.2.75 and BA.4.6 spikes, we only observed significant differences between naive and PI individuals 4 weeks after the third dose (Figures 2D and 2E). Four months after the third dose, we observed a significant decrease of the recognition for naive and PI individuals, with the exception of the BQ.1.1 spike, for which the level remained stable in the PI group (Figures 2A–2F). For the BTI group, the level of recognition remained more stable than for the other groups and reached the same level as the PI group for all tested spikes. We also observed that the BA.4/5 and the BQ.1.1 spikes were always less recognized than the D614G and other Omicron subvariant spikes at both time points for all groups (Figures 2G and 2H).

Neutralizing activity of the vaccine-elicited Abs

We also evaluated the neutralizing activity against pseudoviral particles bearing these spikes in the three groups. Of note, all spikes were incorporated into pseudoviral particles to similar extents (Figure S2C) and had similar levels of infectivity in our assay (Figure S2D). In agreement with the pattern of spike recognition, PI individuals neutralized all the spike variants tested more efficiently than naive individuals 4 weeks after the third dose (Figures 3A–3F). For the BTI group, the level of neutralizing Abs was intermediate between the two other groups. Four months after the third dose, we did not observe significant differences between PI and BTI individuals. In contrast, the naive group neutralized the D614G and Omicron subvariant spikes less efficiently (Figures 3A–3F). Four weeks after the third dose, no significant difference in the level of neutralization was measured between the D614G and BA.2 spikes for the three groups (Figure 2G). In contrast, the other Omicron variant spikes were more resistant to neutralization than the D614G spike in all

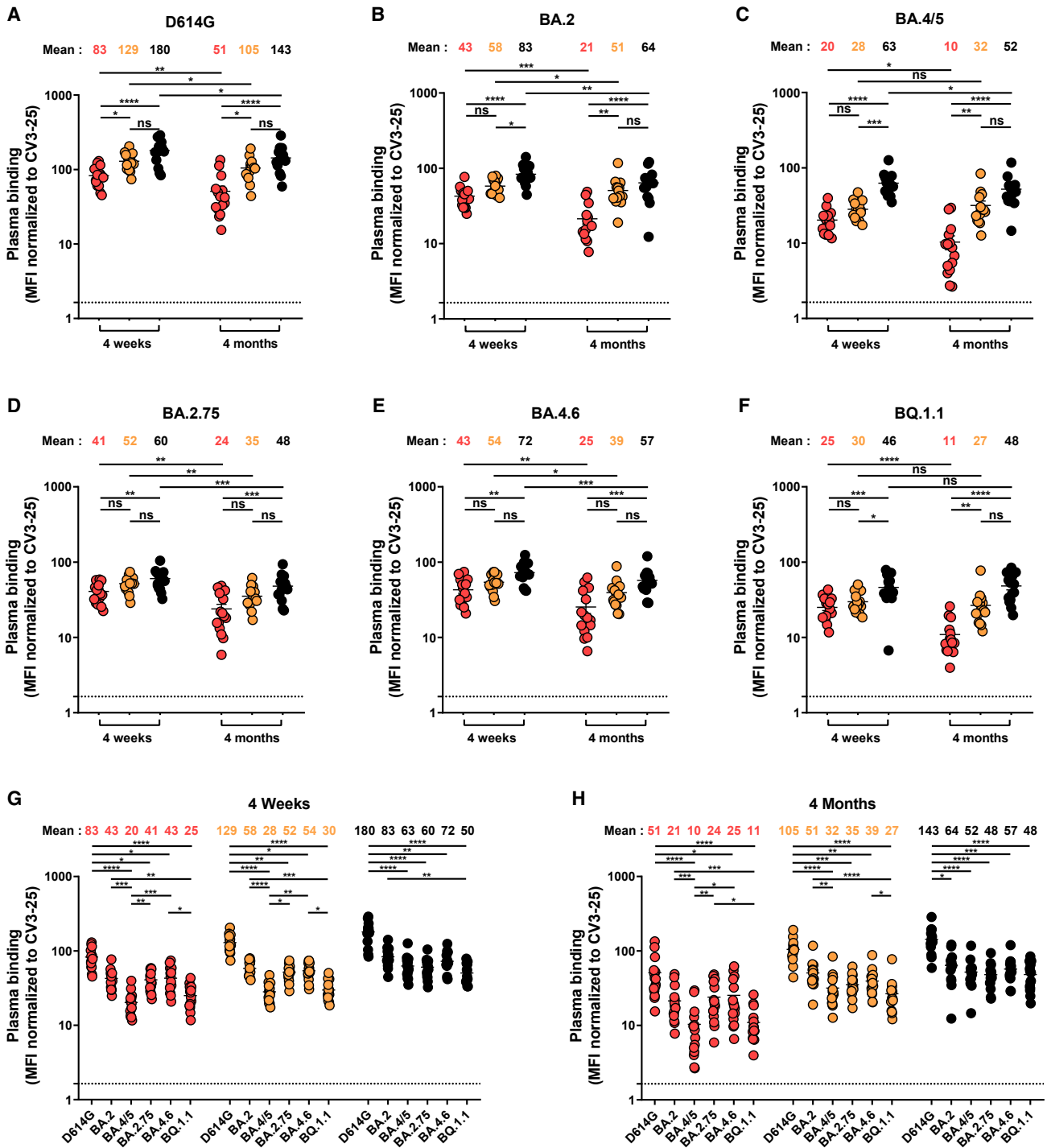


Figure 2. Recognition of SARS-CoV-2 spike variants by plasma from naive, BTI, and PI individuals after the third dose of mRNA vaccine (A–H) 293T cells were transfected with the indicated full-length spike from different SARS-CoV-2 variants and stained with the CV3-25 monoclonal Ab (mAb) or with plasma from naive, BTI, or PI individuals collected 4 weeks or 4 months after the third dose of mRNA vaccine and analyzed by flow cytometry. The values represent the mean fluorescence intensity (MFI) normalized by CV3-25 Ab binding. (A–F) Plasma samples were grouped in two different time points (4 weeks and 4 months) for D614G (A), BA.2 (B), BA.4/5 (C), BA.2.75 (D), BA.4.6 (E), or BQ.1.1 (F) spike recognition. (G and H) Bindings of plasma collected at 4 weeks (G) and 4 months (H) post vaccination were measured. Naive, BTI, and PI individuals are represented by red, yellow, and black points, respectively, undetectable measures are represented as white symbols, and limits of detection are plotted. Error bars indicate means \pm SEM (* p < 0.05; ** p < 0.01; *** p < 0.001; **** p < 0.0001; ns, non-significant). For all groups, n = 15.

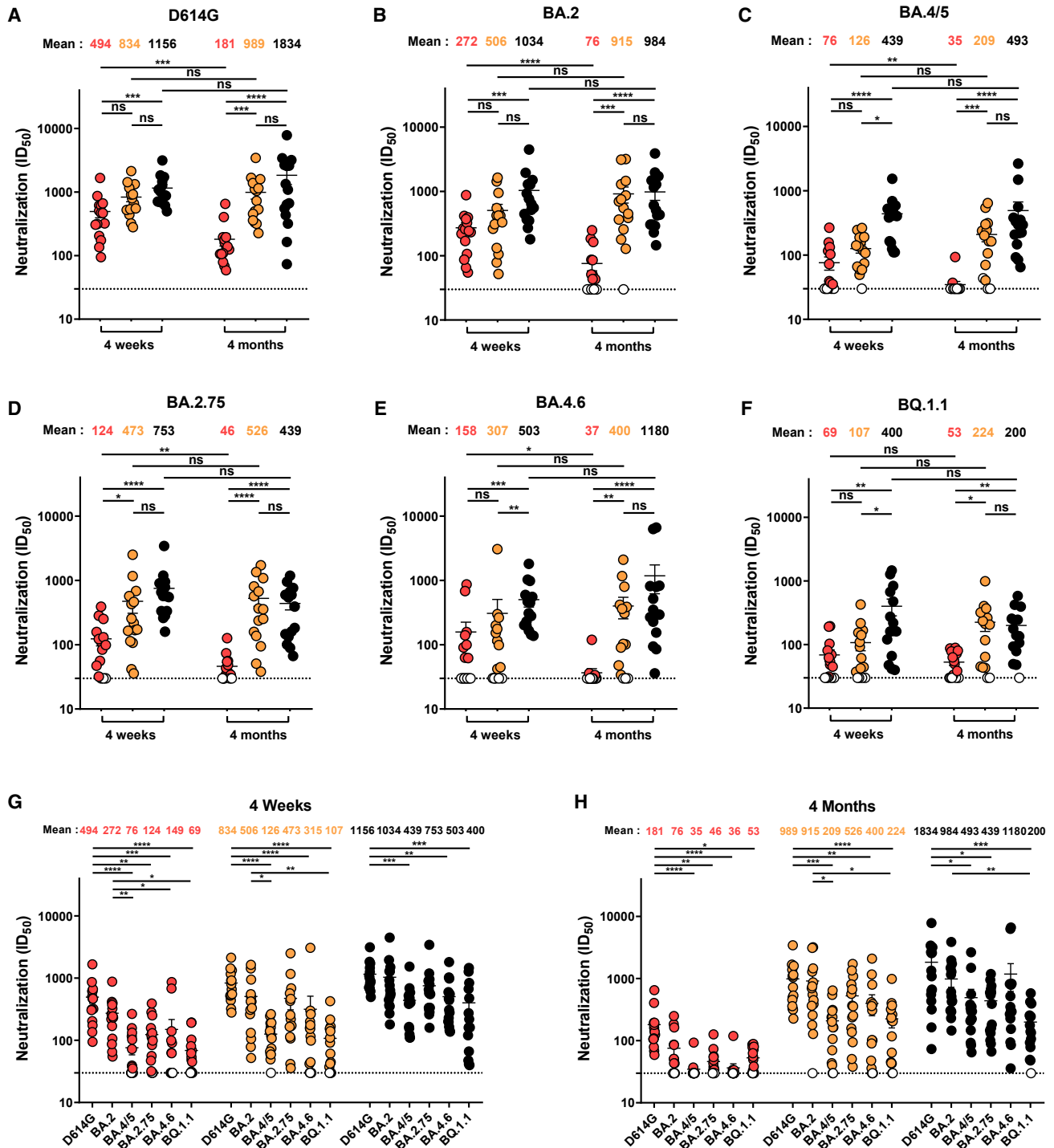


Figure 3. Neutralization activity of SARS-CoV-2 spike variants by plasma from naive, BTI, and PI individuals after the third dose of mRNA vaccine

(A–H) Neutralization activity was measured by incubating pseudoviruses bearing SARS-CoV-2 spike glycoproteins with serial dilutions of plasma for 1 h at 37°C before infecting 293T-ACE2 cells. Neutralization half maximal inhibitory serum dilution (ID₅₀) values were determined using a normalized non-linear regression using GraphPad Prism software.

(legend continued on next page)

groups. Four months after the third dose, weak or no neutralizing activity against Omicron subvariant spikes was detected in most naive individuals (Figures 3B–3F and 3H). For BTI and PI individuals, although neutralizing activity was higher than in naive individuals, the BA.4/5, BA.2.75, BA.4.6, and BQ.1.1 spikes were also significantly less neutralized than the D614G and, in some instances, BA.2 spikes (Figures 3B–3F and 3H).

DISCUSSION

More than 2 years after its emergence, and although an important proportion of the world population has received several doses of vaccine, SARS-CoV-2 variants continue to circulate globally. In recent months, new subvariants of Omicron emerged, carrying an increasing number of mutations and making them more transmissible and resistant to vaccination and monoclonal Ab treatment.^{8,17,20–22,25} In agreement with this, we observed that the BA.4/5, BA.2.75, BA.4.6, and BQ.1.1 spikes were less efficiently recognized and neutralized than the D614G and the BA.2 spikes by plasma from individuals who received three doses of mRNA vaccine.

Several studies reported that poor neutralizing activity against VOCs was observed after two doses of mRNA vaccine, but a third dose strongly improved this response.^{11,16,36} However, when the second dose of vaccine was administered with an extended 16-week interval, higher humoral responses against VOCs (including BA.1 and BA.2) were observed after the second dose of vaccine,¹⁴ which were not increased by a booster dose.¹⁶ Therefore, there is no evidence that additional doses of the original SARS-CoV-2 vaccines after the third dose will result in increased responses against VOCs.

The Omicron variants spread more easily in vaccinated individuals than pre-Omicron variants.^{37,38} Interestingly, it was recently shown that previous infection with an Omicron variant prevents reinfection more efficiently than previous infection with a pre-Omicron variant,^{39,40} thus suggesting that new vaccines based on Omicron variants may generate humoral responses more likely to control Omicron subvariants.

It was previously shown that hybrid immunity due to SARS-CoV-2 infection followed by vaccination confers stronger immune responses than vaccination alone.^{16,32,40,41} Accordingly, here we observed that individuals with BTI had the same level of spike recognition and neutralization as PI individuals, supporting the concept that hybrid protection is similar whatever the order of infection and vaccination. However, the durability of these responses remains unknown.

In conclusion, virus recognition and neutralizing activity induced by current mRNA vaccine are low against Omicron subvariants, rapidly decline over 4 months in naive individuals, and will likely decrease further with future SARS-CoV-2 evolution. There is a need to rapidly develop new generations of vaccines that will elicit broader and less labile protection.

Limitations of the study

One of the limitations of the study is that for most BTI individuals, we do not have the exact day of infection and by which variant. We can only confirm whether they were infected before the first time point studied or between the 2 time points. Furthermore, it is very likely that some PI individuals were exposed a second time. However, in our study, no case of infection was confirmed by PCR in the PI group, and since they were already infected a first time, we cannot conclude that a positive anti-N corresponds to a new infection or to the first. Finally, while we did not observe major differences in infectivity with our pseudoviral particles, it is possible that differences in infectivity and replication exist when using authentic live viruses. For this reason we only report on plasma neutralization profiles, which were shown to be similar between pseudoviral particles and authentic viruses and have been largely used by the field to inform on neutralizing responses elicited by natural infection and vaccination.^{42–46}

STAR★METHODS

Detailed methods are provided in the online version of this paper and include the following:

- KEY RESOURCES TABLE
- RESOURCE AVAILABILITY
 - Lead contact
 - Materials availability
 - Data and code availability
- EXPERIMENTAL MODEL AND SUBJECT DETAILS
 - Ethics statement
 - Human subjects
 - Plasma and antibodies
 - Cell lines
- METHOD DETAILS
 - Plasmids
 - Protein expression and purification
 - Enzyme-linked immunosorbent assay (ELISA) and RBD avidity index
 - SARS-CoV-2-specific B cell characterization
 - Cell surface staining and flow cytometry analysis
 - Pseudoviral infectivity
 - Virus neutralization assay
 - Virus capture assay
- QUANTIFICATION AND STATISTICAL ANALYSIS
 - Statistical analysis

SUPPLEMENTAL INFORMATION

Supplemental information can be found online at <https://doi.org/10.1016/j.celrep.2023.111998>.

(A–F) Plasma samples were grouped in two different time points (4 weeks and 4 months) for D614G (A), BA.2 (B), BA.4/5 (C), BA.2.75 (D), BA.4.6 (E) or BQ.1.1 (F) spike neutralization.

(G and H) Neutralization activity of plasma collected at 4 weeks (G) and 4 months (H) post vaccination were measured.

Naive, BTI, and PI individuals are represented by red, yellow, and black points, respectively, undetectable measures are represented as white symbols, and limits of detection are plotted. Error bars indicate means \pm SEM (* $p < 0.05$; ** $p < 0.01$; *** $p < 0.001$; **** $p < 0.0001$; ns, non-significant). For all groups, $n = 15$.

ACKNOWLEDGMENTS

The authors are grateful to the individuals who participated in this study. The authors thank the CRCHUM BSL3 and Flow Cytometry Platforms for technical assistance. This work was supported by le Ministère de l'Économie et de l'Innovation du Québec, Program de soutien aux organismes de recherche et d'innovation, to A.F. and by the Fondation du CHUM. This work was also supported by a CIHR foundation grant #352417, by a CIHR operating Pandemic and Health Emergencies Research grant #177958, by an Exceptional Fund COVID-19 from the Canada Foundation for Innovation (CFI) #41027 to A.F., and by an FRQS Merit Research Scholar award (#268471) to D.E.K. Work on variants presented was also supported by the Sentinelle COVID Quebec network led by the LSPQ in collaboration with Fonds de Recherche du Québec Santé (FRQS) to A.F. This work was also partially supported by a COVID-19 immunity task force (CITF) grant to A.F. and R.B., by a CIHR COVID-19 rapid response grant (OV3 170632), and a CIHR stream 1 SARS-CoV-2 Variant Research to M.C. A.F. is the recipient of Canada Research Chair on Retroviral Entry no. RCHS0235 950-232424. M.C. is a Tier II Canada Research Chair in Molecular Virology and Antiviral Therapeutics (950-232840). C.T. is the Pfizer/Université de Montréal Chair on HIV translational research. A.T. was supported by a MITACS Accélération postdoctoral fellowship. M.B. was the recipient of a CIHR master's scholarship award. The funders had no role in study design, data collection and analysis, decision to publish, or preparation of the manuscript.

AUTHOR CONTRIBUTIONS

A.T. and A.F. conceived the study. A.T., A.N., S.D., D.C., M.B., K.D., S.Y.G., G.G.-L., H.M., G.G., J.P., Y.B., and A.F. performed, analyzed, and interpreted the experiments. A.T. performed statistical analysis. G.G.-L., H.M., G.G., M.C., and A.F. contributed unique reagents. L.G., P.A., C.M., C.T., and V.M.-L. collected and provided clinical samples. R.B., G.D.S., D.E.K., and I.L. provided scientific input related to VOCs and vaccine efficacy. A.T. and A.F. wrote the manuscript with inputs from others. Every author has read, edited, and approved the final manuscript.

DECLARATION OF INTERESTS

The authors declare no competing interests.

Received: August 3, 2022

Revised: November 28, 2022

Accepted: January 4, 2023

REFERENCES

- Viana, R., Moyo, S., Amoako, D.G., Tegally, H., Scheepers, C., Althaus, C.L., Anyaneji, U.J., Bester, P.A., Boni, M.F., Chand, M., et al. (2022). Rapid epidemic expansion of the SARS-CoV-2 Omicron variant in southern Africa. *Nature* 603, 679–686. <https://doi.org/10.1038/s41586-022-04411-y>.
- WHO Update on Omicron, <https://www.who.int/news/item/28-11-2021-update-on-omicron>. <https://www.who.int/news/item/28-11-2021-update-on-omicron>.
- CDC (2022). COVID data tracker weekly review. *Cent. Dis. Control Prev.* <https://www.cdc.gov/coronavirus/2019-ncov/covid-data/covidview/past-reports/04222022.html>. <https://www.cdc.gov/coronavirus/2019-ncov/covid-data/covidview/past-reports/04222022.html>
- Elliott, P., Eales, O., Steyn, N., Tang, D., Bodinier, B., Wang, H., Elliott, J., Whitaker, M., Atchison, C., Diggle, P.J., et al. (2022). Twin peaks: the omicron SARS-CoV-2 BA.1 and BA.2 epidemics in England. *Science* 376, eabq4411. <https://doi.org/10.1126/science.abq4411>.
- Mohapatra, R.K., Kandi, V., Sarangi, A.K., Verma, S., Tuli, H.S., Chakraborty, S., Chakraborty, C., and Dhama, K. (2022). The recently emerged BA.4 and BA.5 lineages of Omicron and their global health concerns amid the ongoing wave of COVID-19 pandemic – Correspondence. *Int. J. Surg.* 103, 106698. <https://doi.org/10.1016/j.ijisu.2022.106698>.
- PHO (2022). Public Health Ontario : SARS-CoV-2 Omicron Variant Sub-lineages BA.4 and BA.5: Evidence and Risk Assessment, Chrome-Extension. https://efaidnbmnnnibpcajpcglclefindmkaj/https://www.publichealthontario.ca/-/media/Documents/nCoV/voc/2022/07/evidence-brief-ba4-ba5-risk-assessment-jul-8.pdf?sc_lang=en.
- Tegally, H., Moir, M., Everatt, J., Giovanetti, M., Scheepers, C., Wilkinson, E., Subramoney, K., Makatini, Z., Moyo, S., Amoako, D.G., et al. (2022). Emergence of SARS-CoV-2 omicron lineages BA.4 and BA.5 in South Africa. *Nat. Med.* 28, 1785–1790. <https://doi.org/10.1038/s41591-022-01911-2>.
- Yamasoba, D., Kosugi, Y., Kimura, I., Fujita, S., Uriu, K., Ito, J., and Sato, K.; Genotype to Phenotype Japan G2P-Japan Consortium (2022). Neutralisation sensitivity of SARS-CoV-2 omicron subvariants to therapeutic monoclonal antibodies. *Lancet Infect. Dis.* 22, 942–943. [https://doi.org/10.1016/S1473-3099\(22\)00365-6](https://doi.org/10.1016/S1473-3099(22)00365-6).
- WHO (2022). Tracking SARS-CoV-2 Variants. <https://www.who.int/en/activities/tracking-SARS-CoV-2-variants/>. <https://www.who.int/health-topics/typhoid/tracking-SARS-CoV-2-variants>.
- IDSA (2022). SARS-CoV-2 Variants. <https://www.idsociety.org/covid-19-real-time-learning-network/emerging-variants/emerging-covid-19-variants/>. <https://www.idsociety.org/covid-19-real-time-learning-network/emerging-variants/emerging-covid-19-variants/>.
- Muik, A., Lui, B.G., Wallisch, A.-K., Bacher, M., Mühl, J., Reinholz, J., Ozhelvacı, O., Beckmann, N., Güimil Garcia, R.d.I.C., Poran, A., et al. (2022). Neutralization of SARS-CoV-2 Omicron by BNT162b2 mRNA vaccine-elicited human sera. *Science* 375, 678–680. <https://doi.org/10.1126/science.abn7591>.
- Nemet, I., Kliker, L., Lustig, Y., Zuckerman, N., Erster, O., Cohen, C., Kreiss, Y., Alroy-Preis, S., Regev-Yochay, G., Mendelson, E., and Mandelboim, M. (2022). Third BNT162b2 vaccination neutralization of SARS-CoV-2 omicron infection. *N. Engl. J. Med.* 386, 492–494. <https://doi.org/10.1056/NEJMc2119358>.
- Yu, J., Collier, A.R.Y., Rowe, M., Mardas, F., Ventura, J.D., Wan, H., Miller, J., Powers, O., Chung, B., Siamatu, M., et al. (2022). Neutralization of the SARS-CoV-2 omicron BA.1 and BA.2 variants. *N. Engl. J. Med.* 386, 1579–1580. <https://doi.org/10.1056/NEJMc2201849>.
- Chatterjee, D., Tauzin, A., Marchitto, L., Gong, S.Y., Boutin, M., Bourassa, C., Beaudoin-Bussièrès, G., Bo, Y., Ding, S., Laumaea, A., et al. (2022). SARS-CoV-2 Omicron Spike recognition by plasma from individuals receiving BNT162b2 mRNA vaccination with a 16-week interval between doses. *Cell Rep.* 38, 110429. <https://doi.org/10.1016/j.celrep.2022.110429>.
- Payne, R.P., Longet, S., Austin, J.A., Skelly, D.T., Dejnirattisai, W., Adele, S., Mearndon, N., Faustini, S., Al-Taei, S., Moore, S.C., et al. (2021). Immunogenicity of standard and extended dosing intervals of BNT162b2 mRNA vaccine. *Cell* 184, 5699–5714.e11. <https://doi.org/10.1016/j.cell.2021.10.011>.
- Tauzin, A., Gong, S.Y., Chatterjee, D., Ding, S., Painter, M.M., Goel, R.R., Beaudoin-Bussièrès, G., Marchitto, L., Boutin, M., Laumaea, A., et al. (2022). A boost with SARS-CoV-2 BNT162b2 mRNA vaccine elicits strong humoral responses independently of the interval between the first two doses. *Cell Rep.* 41, 111554. <https://doi.org/10.1016/j.celrep.2022.111554>.
- Kurhade, C., Zou, J., Xia, H., Cai, H., Yang, Q., Cutler, M., Cooper, D., Muik, A., Jansen, K.U., Xie, X., et al. (2022). Neutralization of Omicron BA.1, BA.2, and BA.3 SARS-CoV-2 by 3 doses of BNT162b2 vaccine. *Nat. Commun.* 13, 3602. <https://doi.org/10.1038/s41467-022-30681-1>.
- Kitchin, D., Richardson, S.I., van der Mescht, M.A., Motlou, T., Mzindle, N., Moyo-Gwete, T., Makhado, Z., Ayres, F., Manamela, N.P., Spencer, H., et al. (2022). Ad26.COV2.S breakthrough infections induce high titers of neutralizing antibodies against Omicron and other SARS-CoV-2 variants

- of concern. *Cell Rep. Med.* 3, 100535. <https://doi.org/10.1016/j.xcrm.2022.100535>.
19. Miyamoto, S., Arashiro, T., Adachi, Y., Moriyama, S., Kinoshita, H., Kanno, T., Saito, S., Katano, H., Iida, S., Aina, A., et al. (2022). Vaccination-infection interval determines cross-neutralization potency to SARS-CoV-2 Omicron after breakthrough infection by other variants. *Med 3*, 249–261.e4. <https://doi.org/10.1016/j.medj.2022.02.006>.
 20. Qu, P., Faraone, J., Evans, J.P., Zou, X., Zheng, Y.-M., Carlin, C., Bedhash, J.S., Lozanski, G., Mallampalli, R.K., Saif, L.J., et al. (2022). Neutralization of the SARS-CoV-2 omicron BA.4/5 and BA.2.12.1 subvariants. *N. Engl. J. Med.* 386, 2526–2528. <https://doi.org/10.1056/NEJMc2206725>.
 21. Tuekprakhon, A., Nutalai, R., Djokaitė-Guraliuc, A., Zhou, D., Ginn, H.M., Selvaraj, M., Liu, C., Mentzer, A.J., Supasa, P., Duyvesteyn, H.M.E., et al. (2022). Antibody escape of SARS-CoV-2 Omicron BA.4 and BA.5 from vaccine and BA.1 serum. *Cell* 185, 2422–2433.e13. <https://doi.org/10.1016/j.cell.2022.06.005>.
 22. Wang, Q., Guo, Y., Iketani, S., Nair, M.S., Li, Z., Mohri, H., Wang, M., Yu, J., Bowen, A.D., Chang, J.Y., Shah, J.G., Nguyen, N., Chen, Z., Meyers, K., Yin, M.T., Sobieszczyk, M.E., Sheng, Z., Huang, Y., Liu, L., and Ho, D.D. (2022). Antibody evasion by SARS-CoV-2 Omicron Subvariants BA.608.1, BA.4, & BA.5. *Nature* 608, 603–608. <https://doi.org/10.1038/s41586-022-05053-w>.
 23. Shen, X., Chalkias, S., Feng, J., Chen, X., Zhou, H., Marshall, J.-C., Girard, B., Tomassini, J.E., Aunins, A., Das, R., and Montefiori, D.C. (2022). Neutralization of SARS-CoV-2 omicron BA.2.75 after mRNA-1273 vaccination. *N. Engl. J. Med.* 387, 1234–1236. <https://doi.org/10.1056/NEJMc2210648>.
 24. Sheward, D.J., Kim, C., Fischbach, J., Sato, K., Muschiol, S., Ehling, R.A., Björkstöm, N.K., Karlsson Hedestam, G.B., Reddy, S.T., Albert, J., et al. (2022). Omicron sublineage BA.2.75.2 exhibits extensive escape from neutralising antibodies. *Lancet Infect. Dis.* 22, 1538–1540. [https://doi.org/10.1016/S1473-3099\(22\)00663-6](https://doi.org/10.1016/S1473-3099(22)00663-6).
 25. Arora, P., Kempf, A., Nehmeier, I., Schulz, S.R., Jäck, H.M., Pöhlmann, S., and Hoffmann, M. (2023). Omicron sublineage BQ.1.1 resistance to monoclonal antibodies. *Lancet Infect. Dis.* 23, 22–23. [https://doi.org/10.1016/S1473-3099\(22\)00733-2](https://doi.org/10.1016/S1473-3099(22)00733-2).
 26. Kurhade, C., Zou, J., Xia, H., Liu, M., Chang, H.C., Ren, P., Xie, X., and Shi, P.-Y. (2022). Low Neutralization of SARS-CoV-2 Omicron BA.2.75.2, BQ.1.1, and XBB.1 by 4 Doses of Parental mRNA Vaccine or a BA.5-Bivalent Booster. Preprint at bioRxiv. <https://doi.org/10.1101/2022.10.31.514580>.
 27. Tazuin, A., Nayrac, M., Benlarbi, M., Gong, S.Y., Gasser, R., Beaudoin-Bussièrès, G., Brassard, N., Laumaea, A., Vézina, D., Prévost, J., et al. (2021). A single dose of the SARS-CoV-2 vaccine BNT162b2 elicits Fc-mediated antibody effector functions and T cell responses. *Cell Host Microbe* 29, 1137–1150.e6. <https://doi.org/10.1016/j.chom.2021.06.001>.
 28. Tazuin, A., Gong, S.Y., Beaudoin-Bussièrès, G., Vézina, D., Gasser, R., Nault, L., Marchitto, L., Benlarbi, M., Chatterjee, D., Nayrac, M., et al. (2022). Strong humoral immune responses against SARS-CoV-2 Spike after BNT162b2 mRNA vaccination with a 16-week interval between doses. *Cell Host Microbe* 30, 97–109.e5. <https://doi.org/10.1016/j.chom.2021.12.004>.
 29. Prévost, J., Gasser, R., Beaudoin-Bussièrès, G., Richard, J., Duerr, R., Laumaea, A., Anand, S.P., Goyette, G., Benlarbi, M., Ding, S., et al. (2020). Cross-sectional evaluation of humoral responses against SARS-CoV-2 spike. *Cell Rep. Med.* 7, 100126. <https://doi.org/10.1016/j.xcrm.2020.100126>.
 30. Anand, S.P., Prévost, J., Nayrac, M., Beaudoin-Bussièrès, G., Benlarbi, M., Gasser, R., Brassard, N., Laumaea, A., Gong, S.Y., Bourassa, C., et al. (2021). Longitudinal analysis of humoral immunity against SARS-CoV-2 Spike in convalescent individuals up to eight months post-symptom onset. *Cell Rep. Med.*, 100290. <https://doi.org/10.1016/j.xcrm.2021.100290>.
 31. Tazuin, A., Gendron-Lepage, G., Nayrac, M., Anand, S.P., Bourassa, C., Medjahed, H., Goyette, G., Dubé, M., Bazin, R., Kaufmann, D.E., and Finzi, A. (2022). Evolution of anti-RBD IgG avidity following SARS-CoV-2 infection. *Viruses* 14, 532. <https://doi.org/10.3390/v14030532>.
 32. Nayrac, M., Dubé, M., Sannier, G., Nicolas, A., Marchitto, L., Tastet, O., Tazuin, A., Brassard, N., Lima-Barbosa, R., Beaudoin-Bussièrès, G., et al. (2022). Temporal associations of B and T cell immunity with robust vaccine responsiveness in a 16-week interval BNT162b2 regimen. *Cell Rep.* 39, 111013. <https://doi.org/10.1016/j.celrep.2022.111013>.
 33. Li, W., Chen, Y., Prévost, J., Ullah, I., Lu, M., Gong, S.Y., Tazuin, A., Gasser, R., Vézina, D., Anand, S.P., et al. (2022). Structural basis and mode of action for two broadly neutralizing antibodies against SARS-CoV-2 emerging variants of concern. *Cell Rep.* 38, 110210. <https://doi.org/10.1016/j.celrep.2021.110210>.
 34. Prévost, J., Richard, J., Gasser, R., Ding, S., Fage, C., Anand, S.P., Adam, D., Gupta Vergara, N., Tazuin, A., Benlarbi, M., et al. (2021). Impact of temperature on the affinity of SARS-CoV-2 Spike glycoprotein for host ACE2. *J. Biol. Chem.* 297, 101151. <https://doi.org/10.1016/j.jbc.2021.101151>.
 35. Ullah, I., Prévost, J., Ladinsky, M.S., Stone, H., Lu, M., Anand, S.P., Beaudoin-Bussièrès, G., Symmes, K., Benlarbi, M., Ding, S., et al. (2021). Live imaging of SARS-CoV-2 infection in mice reveals that neutralizing antibodies require Fc function for optimal efficacy. *Immunity* 54, 2143–2158.e15. <https://doi.org/10.1016/j.immuni.2021.08.015>.
 36. Gruell, H., Vanshylla, K., Tober-Lau, P., Hillus, D., Schommers, P., Lehmann, C., Kurth, F., Sander, L.E., and Klein, F. (2022). mRNA booster immunization elicits potent neutralizing serum activity against the SARS-CoV-2 Omicron variant. *Nat. Med.* 28, 477–480. <https://doi.org/10.1038/s41591-021-01676-0>.
 37. Garrett, N., Tapley, A., Andriesen, J., Seocharan, I., Fisher, L.H., Bunts, L., Espy, N., Wallis, C.L., Randhawa, A.K., Ketter, N., et al. (2022). High rate of asymptomatic carriage associated with variant strain omicron. Preprint at medRxiv. <https://doi.org/10.1101/2021.12.20.21268130>.
 38. Sun, K., Tempia, S., Kleynhans, J., von Gottberg, A., McMorro, M.L., Wolter, N., Bhiman, J.N., Moyes, J., du Plessis, M., Carrim, M., et al. (2022). SARS-CoV-2 transmission, persistence of immunity, and estimates of Omicron's impact in South African population cohorts. *Sci. Transl. Med.* 14, eabo7081. <https://doi.org/10.1126/scitranslmed.abo7081>.
 39. Altarawneh, H.N., Chemaitelly, H., Ayoub, H.H., Hasan, M.R., Coyle, P., Yassine, H.M., Al-Khatib, H.A., Benslimane, F.M., Al-Kanaani, Z., Al-Kuwari, E., et al. (2022). Protection of SARS-CoV-2 Natural Infection against Reinfection with the Omicron BA.4 or BA.5 Subvariants. Preprint at medRxiv. <https://doi.org/10.1101/2022.07.11.22277448>.
 40. Carazo, S., Skowronski, D.M., Brisson, M., Sauvageau, C., Brousseau, N., Gilca, R., Ouakki, M., Barkati, S., Fafard, J., Talbot, D., et al. (2022). Protection against Omicron Re-infection Conferred by Prior Heterologous SARS-CoV-2 Infection, with and without mRNA Vaccination. Preprint at medRxiv. <https://doi.org/10.1101/2022.04.29.22274455>.
 41. Goel, R.R., Apostolidis, S.A., Painter, M.M., Mathew, D., Pattekar, A., Kuthuru, O., Gouma, S., Hicks, P., Meng, W., Rosenfeld, A.M., et al. (2021). Distinct antibody and memory B cell responses in SARS-CoV-2 naïve and recovered individuals following mRNA vaccination. *Sci. Immunol.* 6, eabi6950. <https://doi.org/10.1126/sciimmunol.abi6950>.
 42. Valcourt, E.J., Manguiat, K., Robinson, A., Lin, Y.-C., Abe, K.T., Mubareka, S., Shigayeva, A., Zhong, Z., Girardin, R.C., DuPuis, A., et al. (2021). Evaluating humoral immunity against SARS-CoV-2: validation of a plaque-reduction neutralization test and a multilaboratory comparison of conventional and surrogate neutralization assays. *Microbiol. Spectr.* 9, e0088621. <https://doi.org/10.1128/Spectrum.00886-21>.
 43. Sun, H., Xu, J., Zhang, G., Han, J., Hao, M., Chen, Z., Fang, T., Chi, X., and Yu, C. (2022). Developing pseudovirus-based neutralization assay against omicron-included SARS-CoV-2 variants. *Viruses* 14, 1332. <https://doi.org/10.3390/v14061332>.

44. Wang, Z., Muecksch, F., Muenn, F., Cho, A., Zong, S., Raspe, R., Ramos, V., Johnson, B., Ben Tanfous, T., DaSilva, J., et al. (2022). Humoral immunity to SARS-CoV-2 elicited by combination COVID-19 vaccination regimens. *J. Exp. Med.* 219, e20220826. <https://doi.org/10.1084/jem.20220826>.
45. Schmidt, F., Muecksch, F., Weisblum, Y., Da Silva, J., Bednarski, E., Cho, A., Wang, Z., Gaebler, C., Caskey, M., Nussenzweig, M.C., et al. (2022). Plasma neutralization of the SARS-CoV-2 omicron variant. *N. Engl. J. Med.* 386, 599–601. <https://doi.org/10.1056/NEJMc2119641>.
46. Robbiani, D.F., Gaebler, C., Muecksch, F., Lorenzi, J.C.C., Wang, Z., Cho, A., Agudelo, M., Barnes, C.O., Gazumyan, A., Finkin, S., et al. (2020). Convergent antibody responses to SARS-CoV-2 in convalescent individuals. *Nature* 584, 437–442. <https://doi.org/10.1038/s41586-020-2456-9>.
47. Jennewein, M.F., MacCamy, A.J., Akins, N.R., Feng, J., Homad, L.J., Hurlburt, N.K., Seydoux, E., Wan, Y.-H., Stuart, A.B., Edara, V.V., et al. (2021). Isolation and characterization of cross-neutralizing coronavirus antibodies from COVID-19+ subjects. *Cell Rep.* 36, 109353. <https://doi.org/10.1016/j.celrep.2021.109353>.
48. Beaudoin-Bussi eres, G., Laumaea, A., Anand, S.P., Pr evost, J., Gasser, R., Goyette, G., Medjahed, H., Perreault, J., Tremblay, T., Lewin, A., et al. (2020). Decline of humoral responses against SARS-CoV-2 spike in convalescent individuals. *mBio* 11, e02590-20. <https://doi.org/10.1128/mBio.02590-20>.
49. Gong, S.Y., Chatterjee, D., Richard, J., Pr evost, J., Tauzin, A., Gasser, R., Bo, Y., V ezina, D., Goyette, G., Gendron-Lepage, G., et al. (2021). Contribution of single mutations to selected SARS-CoV-2 emerging variants spike antigenicity. *Virology* 563, 134–145. <https://doi.org/10.1016/j.virol.2021.09.001>.
50. Ding, S., Laumaea, A., Benlarbi, M., Beaudoin-Bussi eres, G., Gasser, R., Medjahed, H., Pancera, M., Stamatatos, L., McGuire, A.T., Bazin, R., and Finzi, A. (2020). Antibody binding to SARS-CoV-2 S glycoprotein correlates with but does not predict neutralization. *Viruses* 12, 1214. <https://doi.org/10.3390/v12111214>.

STAR★METHODS

KEY RESOURCES TABLE

REAGENT or RESOURCE	SOURCE	IDENTIFIER
Antibodies		
LIVE-DEAD Fixable AquaVivid Cell Stain	Thermo Fisher Scientific	Cat# P34957
CV3-25 monoclonal antibody	Jennewein et al., 2021 ⁴⁷	N/A
CR3022 monoclonal antibody	Dr M. Gordon Joyce	RRID: AB_2848080
Alexa Fluor 647 AffiniPure Goat Anti-Human IgA + IgG + IgM (H + L)	Jackson ImmunoResearch	Cat # 109-605-064; RRID: AB_2337886
UCHT1 (BV480) [anti-human CD3]	BD Biosciences	Cat# 566105; RRID: AB_2739507
M5E2 (BV480) [anti-human CD14]	BD Biosciences	Cat#746304; RRID: AB_2743629
3G8 (BV480) [anti-human CD16]	BD Biosciences	Cat# 566108; RRID: AB_2739510
SJ25C1 (BV650) [anti-human CD19]	Biolegend	Cat# 363026; RRID: AB_2564255
2H7 (BV711) [anti-human CD20]	Biolegend	Cat# 302342; RRID: AB_2562602
B-LY4 (BV789) [anti-human CD21]	BD Biosciences	Cat# 740969; RRID: AB_2740594)
ML5 (BUV805) [anti-human CD24]	BD Biosciences	Cat# 742010; RRID: AB_2871308
M-T271 (APC-R700) [anti-human CD27]	BD Biosciences	Cat# 565116; RRID: AB_2739074
HIT2 (BB790) [anti-human CD38]	BD Biosciences	N/A
NCAM16.2 (BV480) [anti-human CD56]	BD Biosciences	Cat# 566124; RRID: AB_2739525
MI15 (BUV661) [anti-human CD138]	BD Biosciences	Cat# 749873; RRID: AB_2874113
1B5 (BUV395) [anti-human CCR10]	BD Biosciences	Cat# 565322; RRID: AB_2739181
G46-6 (BB700) [anti-human HLA-DR]	BD Biosciences	Cat# 566480; RRID: AB_2744477
IS11-8E10 (PE) [anti-human IgA]	Miltenyi Biotec	Cat# 130-113-476; RRID: AB_2733861
IA6-2 (BUV563) [anti-human IgD]	BD Biosciences	Cat# 741394; RRID: AB_2870889
G18-147 (BV421) [anti-human IgG]	BD Biosciences	Cat# 562581; RRID: AB_2737665
UCH-B1 (BUV737 [anti-human IgM]	BD Biosciences	Cat# 748928; RRID: AB_2873331
Biological samples		
SARS-CoV-2 naive donor blood samples	This paper	N/A
SARS-CoV-2 breakthrough infection donor blood samples	This paper	N/A
SARS-CoV-2 previously infected donor blood samples	This paper	N/A
Chemicals, peptides, and recombinant proteins		
Dulbecco's Modified Eagle's medium (DMEM)	Wisent	Cat# 319-005-CL
Roswell Park Memorial Institute (RPMI)	Thermo Fisher Scientific	Cat# 72400120
Penicillin/Streptomycin	Wisent	Cat# 450-201-EL
Fetal Bovine Serum (FBS)	VWR	Cat# 97068-085
Phosphate Buffered Saline (PBS)	Thermo Fisher Scientific	Cat# 10010023
BSA	Sigma	Cat# A7638
Tween 20	Sigma	Cat# P9416-100ML
Puromycin Dihydrochloride	Millipore Sigma	Cat# P8833
Passive Lysis Buffer	Promega	Cat# E1941
D-Luciferin Potassium Salt	Thermo Fisher Scientific	Cat# L2916
Freestyle 293F expression medium	Thermo Fisher Scientific	Cat# A14525
Western Lightning Plus-ECL, Enhanced Chemiluminescence Substrate	Perkin Elmer Life Sciences	Cat# NEL105001EA
Formaldehyde 37%	Thermo Fisher Scientific	Cat# F79-500

(Continued on next page)

Continued		
REAGENT or RESOURCE	SOURCE	IDENTIFIER
Experimental models: Cell lines		
HEK293T cells	ATCC	Cat# CRL-3216; RRID: CVCL_0063
293T-ACE2 cells	Prévost et al., 2020 ²⁹	N/A
FreeStyle 293F cells	Thermo Fisher Scientific	Cat# R79007; RRID: CVCL_D603
Cf2.Th cells	ATCC	Cat# CRL-1430; RRID:CVCL_3363
Recombinant DNA		
pNL4.3 R-E– Luc	NIH AIDS reagent program	Cat# 3418
pIRES2-EGFP	Clontech	Cat# 6029-1
pCG1-SARS-CoV-2 D614G-Spike	Beaudoin-Bussières et al., 2020 ⁴⁸	N/A
pCAGGS-SARS-CoV-2-BA.2 Spike	Tauzin et al., 2022 ¹⁶	N/A
pCAGGS-SARS-CoV-2-BA.4/5 Spike	This paper	N/A
pCAGGS-SARS-CoV-2-BA.2.75 Spike	This paper	N/A
pCAGGS-SARS-CoV-2-BA.4.6 Spike	This paper	N/A
pCAGGS-SARS-CoV-2-BQ.1.1 Spike	This paper	N/A
pSVMV-IN-VSV-G	Prévost et al., 2020 ²⁹	N/A
Software and algorithms		
Flow Jo v10.7.1	Flow Jo	https://www.flowjo.com
GraphPad Prism v8.4.3	GraphPad	https://www.graphpad.com
Microsoft Excel v16	Microsoft Office	https://www.microsoft.com/en-ca/microsoft-365/excel
Others		
BD LSRII Flow Cytometer	BD Biosciences	N/A
Symphony cytometer	BD Biosciences	N/A
TriStar LB942 Microplate Reader	Berthold Technologies	N/A

RESOURCE AVAILABILITY

Lead contact

Further information and requests for resources and reagents should be directed to and will be fulfilled by the lead contact, Andrés Finzi (andres.finzi@umontreal.ca).

Materials availability

All unique reagents generated during this study are available from the [lead contact](#) without restriction.

Data and code availability

- All data reported in this paper will be shared by the [lead contact](#) (andres.finzi@umontreal.ca) upon request.
- This paper does not report original code.
- Any additional information required to reanalyze the data reported in this paper is available from the [lead contact](#) (andres.finzi@umontreal.ca) upon request.

EXPERIMENTAL MODEL AND SUBJECT DETAILS

Ethics statement

All work was conducted in accordance with the Declaration of Helsinki in terms of informed consent and approval by an appropriate institutional board. Blood samples were obtained from donors who consented to participate in this research project at CHUM (19.381). Plasmas and PBMCs were isolated by centrifugation and Ficoll gradient, and samples stored at -80°C and in liquid nitrogen respectively, until use.

Human subjects

The study was conducted in 15 SARS-CoV-2 naive individuals (4 males and 11 females; age range: 24–67 years), 15 SARS-CoV-2 breakthrough infection individuals (5 males and 10 females; age range: 30–64 years) infected after the second or third dose of

mRNA vaccine (6 BTI were infected before the time point collected 4 weeks after the third dose and 9 individuals were infected between the two time points), and 15 SARS-CoV-2 previously infected individuals (8 males and 7 females; age range: 29-65 years) infected before vaccination during the first wave of COVID-19 in March-May 2020. This information is presented in [Table 1](#). No specific criteria such as number of patients (sample size), gender, clinical or demographic were used for inclusion, beyond PCR confirmed SARS-CoV-2 infection in adults before vaccination for PI group, PCR confirmed SARS-CoV-2 infection or anti-N positive in adults after vaccination for BTI group and no detection of Abs recognizing the N protein for naive individuals.

Plasma and antibodies

Plasmas were isolated by centrifugation with Ficoll gradient, heat-inactivated for 1 h at 56°C and stored at –80°C until use in subsequent experiments. Healthy donor's plasmas, collected before the pandemic, were used as negative controls, and used to calculate the seropositivity threshold in our ELISAs and flow cytometry assays (data not shown). The RBD-specific monoclonal antibody CR3022 was used as a positive control in ELISA assays, and the conformationally independent S2-specific monoclonal antibody CV3-25 was used as a positive control and to normalize spike expression in our flow cytometry assays, as described.^{28,34,47,49} Horseradish peroxidase (HRP)-conjugated Abs able to detect the Fc region of human IgG (Invitrogen) was used as secondary Abs to detect Ab binding in ELISA experiments. Alexa Fluor-647-conjugated goat anti-human Abs able to detect all Ig isotypes (anti-human IgM+IgG+IgA; Jackson ImmunoResearch Laboratories) were used as secondary Abs to detect plasma binding in flow cytometry experiments.

Cell lines

293T human embryonic kidney cells (obtained from ATCC) and Cf2.Th cells (a kind gift from Joseph Sodroski, Dana Farber Cancer Institute (DFCI), Boston, MA, USA) were maintained at 37°C under 5% CO₂ in Dulbecco's modified Eagle's medium (DMEM) (Wisent) containing 5% fetal bovine serum (FBS) (VWR) and 100 µg/mL of penicillin-streptomycin (Wisent). 293T-ACE2 cell line was previously reported.²⁹

METHOD DETAILS

Plasmids

The plasmids encoding the SARS-CoV-2 spike variants were previously described.^{16,48,49} The plasmids encoding the BA.4/5, BA.2.75, BA.4.6 and BQ.1.1 spikes were generated by overlapping PCR using the BA.2 SARS-CoV-2 spike gene as a template and cloned in pCAGGS. All constructs were verified by Sanger sequencing. Spike variant sequences are outlined in [Figure S2A](#). The pNL4.3 R-E–Luc was obtained from the NIH AIDS Reagent Program. The vesicular stomatitis virus G (VSV-G)-encoding plasmid (pSVMV-IN-VSV-G) was previously described.²⁹

Protein expression and purification

FreeStyle 293F cells (Invitrogen) were grown in FreeStyle 293F medium (Invitrogen) to a density of 1×10^6 cells/mL at 37°C with 8% CO₂ with regular agitation (150 rpm). Cells were transfected with a plasmid coding for SARS-CoV-2 S WT RBD⁴⁸ using ExpiFectamine 293 transfection reagent, as directed by the manufacturer (Invitrogen). One week later, cells were pelleted and discarded. Supernatants were filtered using a 0.22 µm filter (Thermo Fisher Scientific). The recombinant RBD proteins were purified by nickel affinity columns, as directed by the manufacturer (Invitrogen). The RBD preparations were dialyzed against phosphate-buffered saline (PBS) and stored in aliquots at –80°C until further use. To assess purity, recombinant proteins were loaded on SDS-PAGE gels and stained with Coomassie Blue.

Enzyme-linked immunosorbent assay (ELISA) and RBD avidity index

The SARS-CoV-2 WT RBD ELISA assay used was previously described.^{29,48} Briefly, recombinant SARS-CoV-2 WT RBD proteins (2.5 mg/mL), or BSA (2.5 mg/mL) as a negative control, were prepared in PBS and were adsorbed to plates (MaxiSorp Nunc) overnight at 4°C. Coated wells were subsequently blocked with blocking buffer (Tris-buffered saline [TBS] containing 0.1% Tween 20 and 2% BSA) for 1h at room temperature. Wells were then washed four times with washing buffer (Tris-buffered saline [TBS] containing 0.1% Tween 20). CR3022 mAb (50 ng/mL) or a 1/500 dilution of plasma were prepared in a diluted solution of blocking buffer (0.1% BSA) and incubated with the RBD-coated wells for 90 min at room temperature. Plates were washed four times with washing buffer followed by incubation with secondary Abs (diluted in a diluted solution of blocking buffer (0.4% BSA)) for 1h at room temperature, followed by four washes. To calculate the RBD-avidity index, we performed in parallel a stringent ELISA, where the plates were washed with a chaotropic agent, 8M of urea, added of the washing buffer. This assay was previously described.³¹ HRP enzyme activity was determined after the addition of a 1:1 mix of Western Lightning oxidizing and luminol reagents (PerkinElmer Life Sciences). Light emission was measured with an LB942 TriStar luminometer (Berthold Technologies). Signal obtained with BSA was subtracted for each plasma and was then normalized to the signal obtained with CR3022 present in each plate. The seropositivity threshold was established using the following formula: mean of pre-pandemic SARS-CoV-2 negative plasma + (3 standard deviation of the mean of pre-pandemic SARS-CoV-2 negative plasma).

SARS-CoV-2-specific B cell characterization

To detect SARS-CoV-2-specific B cells, we conjugated recombinant RBD proteins with Alexa Fluor 488 or Alexa Fluor 594 (Thermo Fisher Scientific) according to the manufacturer's protocol. 2×10^6 frozen PBMCs from SARS-CoV-2 naive, BTI and PI donors were prepared at a final concentration of 4×10^6 cells/mL in RPMI 1640 medium (GIBCO) supplemented with 10% of fetal bovine serum (Seradigm), Penicillin/Streptomycin (GIBCO) and HEPES (GIBCO). After a rest of 2h at 37°C and 5% CO₂, cells were stained using Aquavid viability marker (GIBCO) in DPBS (GIBCO) at 4°C for 20 min. The detection of SARS-CoV-2-antigen specific B cells was done by adding the RBD probes to the antibody cocktail listed in [Table S1](#). Staining was performed at 4°C for 30 min and cells were fixed using 2% paraformaldehyde at 4°C for 15 min. Stained PBMC samples were acquired on Symphony cytometer (BD Biosciences) and analyzed using FlowJo v10.8.0 software and the gating strategy presented in [Figure S1A](#).

Cell surface staining and flow cytometry analysis

293T were transfected with full-length SARS-CoV-2 spikes and a green fluorescent protein (GFP) expressor (pIRES2-eGFP; Clontech) using the calcium-phosphate method. Two days post-transfection, spike-expressing 293T cells were stained with the CV3-25 Ab (5 µg/mL) as control or plasma from naive, BTI or PI individuals (1:250 dilution) for 45 min at 37°C. AlexaFluor-647-conjugated goat anti-human IgG (1/1000 dilution) were used as secondary Abs. The percentage of spike-expressing cells (GFP + cells) was determined by gating the living cell population based on viability dye staining (Aqua Vivid, Invitrogen). Samples were acquired on an LSR II cytometer (BD Biosciences), and data analysis was performed using FlowJo v10.7.1 (Tree Star) using the gating strategy presented in [Figure S1B](#). The conformationally-independent anti-S2 antibody CV3-25 was used to normalize spike expression, as reported.^{33–35,49} CV3-25 was shown to be effective against all spike variants ([Figures S2B and S2C](#)). The Median Fluorescence intensities (MFI) obtained with plasma were normalized to the MFI obtained with CV3-25 and presented as percentage of CV3-25 binding.

Pseudoviral infectivity

293T cells were transfected with the lentiviral vector pNL4.3 R-E– Luc (NIH AIDS Reagent Program) and plasmid encoding for the indicated spike glycoprotein (D614G, BA.2, BA.4/5, BA.2.75, BA.4.6 or BQ.1.1) at a ratio of 10:1. Two days post-transfection, cell supernatants were harvested and stored at –80°C until use. The RT activity was evaluated by measure of the incorporation of [*methyl*-3H]TTP into cDNA of a poly(rA) template in the presence of virion-associated RT and oligo(dT). Normalized amount of RT activity pseudoviral particles were added to 293T-ACE2 target cells for 48 h at 37°C. Then, cells were lysed by the addition of 30 µL of passive lysis buffer (Promega) followed by one freeze-thaw cycle. An LB942 TriStar luminometer (Berthold Technologies) was used to measure the luciferase activity of each well after the addition of 100 µL of luciferin buffer (15mM MgSO₄, 15mM KPO₄ [pH 7.8], 1mM ATP, and 1mM dithiothreitol) and 50 µL of 1mM d-luciferin potassium salt (Thermo Fisher Scientific). RLU values obtained were normalized to D614G.

Virus neutralization assay

To produce SARS-CoV-2 pseudoviruses, 293T cells were transfected with the lentiviral vector pNL4.3 R-E– Luc (NIH AIDS Reagent Program) and a plasmid encoding for the indicated spike glycoprotein (D614G, BA.2, BA.4/5, BA.2.75, BA.4.6 or BQ.1.1) at a ratio of 10:1. Two days post-transfection, cell supernatants were harvested and stored at –80°C until use. For the neutralization assay, 293T-ACE2 target cells were seeded at a density of 1×10^4 cells/well in 96-well luminometer-compatible tissue culture plates (PerkinElmer) 24h before infection. Pseudoviral particles were incubated with several plasma dilutions (1/50; 1/250; 1/1250; 1/6250; 1/31,250) for 1h at 37°C and were then added to the target cells followed by incubation for 48 h at 37°C. Cells were lysed by the addition of 30 µL of passive lysis buffer (Promega) followed by one freeze-thaw cycle. An LB942 TriStar luminometer (Berthold Technologies) was used to measure the luciferase activity of each well after the addition of 100 µL of luciferin buffer (15mM MgSO₄, 15mM KH₂PO₄ [pH 7.8], 1mM ATP, and 1mM dithiothreitol) and 50 µL of 1mM d-luciferin potassium salt (Prolume). The neutralization half-maximal inhibitory dilution (ID₅₀) represents the plasma dilution to inhibit 50% of the infection of 293T-ACE2 cells by pseudoviruses.

Virus capture assay

The assay was previously described.⁵⁰ Briefly, pseudoviral particles were produced by transfecting 2×10^6 293T cells with pNL4.3 R-E– Luc (3.5 µg), pSVCMV-IN-VSV-G (1 µg) and plasmids encoding for SARS-CoV-2 spike glycoproteins (3.5 µg) using the standard calcium phosphate protocol. 48 h later, virion-containing supernatants were collected. White MaxiSorp ELISA plates (Thermo Fisher Scientific, Waltham, MA, USA) were plated with the CV3-25 mAb at 0.05 µg per well overnight at 4°C. Unbound antibodies were removed by washing the plates twice with PBS. Plates were subsequently blocked with 3% BSA in PBS for 1 h at room temperature. After the washes, 200 µL of virus-containing supernatant was added to the wells. Viral capture by the Ab was visualized by adding 1×10^4 SARS-CoV-2-resistant Cf2Th cells in full DMEM medium per well. Forty-eight hours post-infection, cells were lysed by the addition of 30 µL of passive lysis buffer (Promega, Madison, WI, USA.) and three freeze-thaw cycles. An LB941 TriStar luminometer (Berthold Technologies) was used to measure the luciferase activity of each well after the addition of 100 µL of luciferin buffer (15mM MgSO₄, 15mM KH₂PO₄ (pH 7.8), 1mM ATP, and 1mM dithiothreitol) and 50 µL of 1mM D-luciferin potassium salt (Prolume, Randolph, VT, USA.).

QUANTIFICATION AND STATISTICAL ANALYSIS

Statistical analysis

Symbols represent biologically independent samples from SARS-CoV-2 naive, BTI or PI individuals. Statistics were analyzed using GraphPad Prism version 8.0.1 (GraphPad, San Diego, CA). Every dataset was tested for statistical normality and this information was used to apply the appropriate (parametric or nonparametric) statistical test. p values <0.05 were considered significant; significance values are indicated as *p < 0.05, **p < 0.01, ***p < 0.001, ****p < 0.0001, ns, non-significant.